Extraordinary Flood Response of a Small Urban Watershed to Short-Duration Convective Rainfall

JAMES A. SMITH

Department of Civil and Environmental Engineering, Princeton University, Princeton, New Jersey

ANDREW J. MILLER

Department of Geography and Environmental Systems, University of Maryland, Baltimore County, Baltimore, Maryland

MARY LYNN BAECK AND PETER A. NELSON

Department of Civil and Environmental Engineering, Princeton University, Princeton, New Jersey

GARY T. FISHER

U. S. Geological Survey, Baltimore, Maryland

KATHERINE L. MEIERDIERCKS

Department of Civil and Environmental Engineering, Princeton University, Princeton, New Jersey

(Manuscript received 3 August 2004, in final form 5 January 2005)

ABSTRACT

The 9.1 km^2 Moores Run watershed in Baltimore, Maryland, experiences floods with unit discharge peaks exceeding 1 m^3 s^{-1} km^{-2} 12 times yr^{-1}, on average. Few, if any, drainage basins in the continental United States have a higher frequency. A thunderstorm system on 13 June 2003 produced the record flood peak (13.2 m^3 s^{-1} km^{-2}) during the 6-yr stream gauging record of Moores Run. In this paper, the hydrometeorology, hydrology, and hydraulics of extreme floods in Moores Run are examined through analyses of the 13 June 2003 storm and flood, as well as other major storm and flood events during the 2000–03 time period. The 13 June 2003 flood, like most floods in Moores Run, was produced by an organized system of thunderstorms. Analyses of the 13 June 2003 storm, which are based on volume scan reflectivity observations from the Sterling, Virginia, WSR-88D radar, are used to characterize the spatial and temporal variability of flash flood producing rainfall. Hydrology of flood response in Moores Run is characterized by highly efficient concentration of runoff through the storm drain network and relatively low runoff ratios. A detailed survey of high-water marks for the 13 June 2003 flood is used, in combination with analyses based on a 2D, depth-averaged open channel flow model (TELEMAC 2D) to examine hydraulics of the 13 June 2003 flood. Hydraulic analyses are used to examine peak discharge estimates for the 13 June flood peak, propagation of flood waves in the Moores Run channel, and 2D flow features associated with channel and floodplain geometry.

1. Introduction

Flood peaks exceeding 1 m^3 s^{-1} km^{-2} in the Moores Run watershed in Baltimore, Maryland (Fig. 1), have a return interval of approximately 1 month, one of the highest frequencies in the conterminous United States. A thunderstorm system on 13 June 2003 produced the record flood peak during the 6-yr stream gauging record of Moores Run. Peak discharge estimates for the 13 June flood (see section 3) range from 120 to 230 m^3 s^{-1} for the 9.1 km^2 basin, resulting in unit discharge peaks ranging from 13.2 to 25.2 m^3 s^{-1} km^{-2}. In this paper, we examine the hydrometeorology, hydrology, and hydraulics of extreme floods in Moores Run through analyses of the 13 June 2003 storm and flood, as well as

Corresponding author address: Dr. James A. Smith, Dept. of Civil and Environmental Engineering, Princeton University, Princeton, NJ 08540.
E-mail: jsmith@princeton.edu

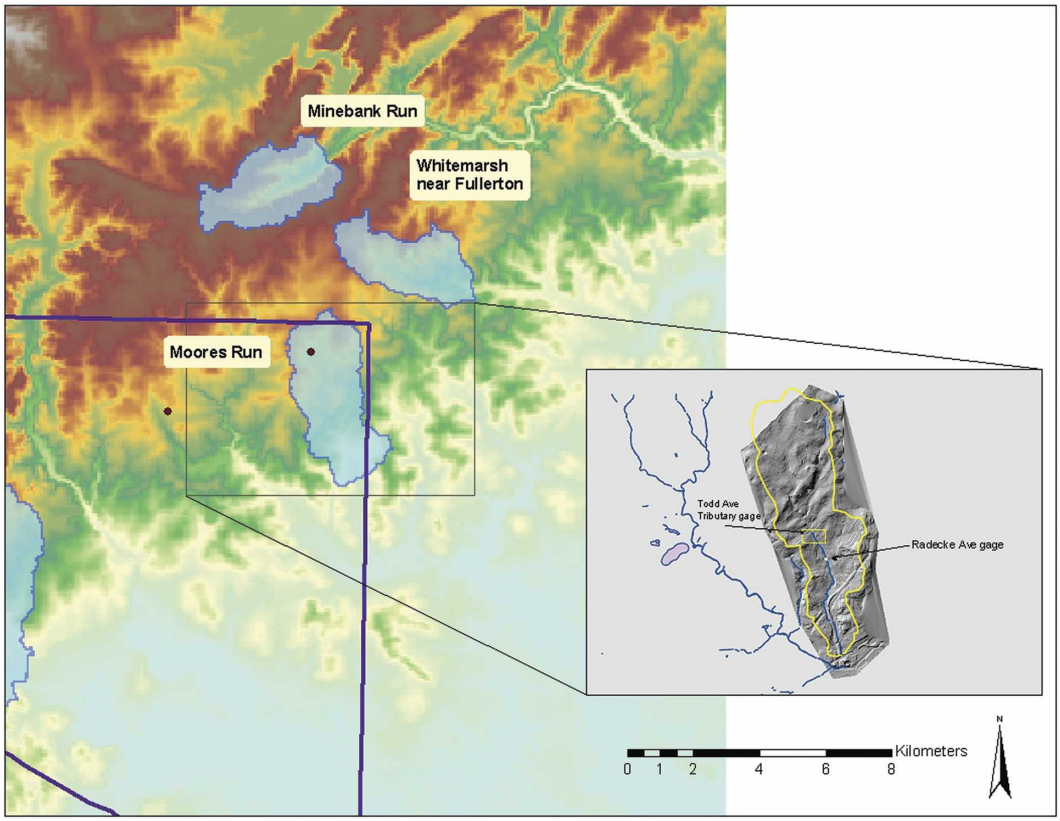

FIG. 1. Overview image with DEM, basin boundaries, and observing sites. Inset of Moores Run drainage basin shows surface channel and locations of stream gauging stations. Locations of rain gauges RG2 and RG5 are shown as solid black dots (RG2 is within the Moores Run basin and RG5 is west of the rectangular inset region).

other major storm and flood events during the 2000–03 time period. As an "end member" in the flood response spectrum of U. S. catchments, analyses of Moores Run response provide insights into the processes that produce extreme floods in urban drainage basins.

The U. S. Geological Survey (USGS) operates stream gauging stations on Moores Run (Fig. 1) at the Radecke Avenue Bridge (drainage area of 9.1 km^2) and at Todd Avenue (0.54 km^2). Moores Run is an urbanized watershed dominated by dense residential land use. Development of the basin occurred more than 100 years ago and by the mid-1930s the surface drainage system consisted of a single channel in the lower drainage basin (Fig. 1). The Radecke Avenue gauge is less than 500 m downstream of the storm drain outfall that marks the origin of the existing surface drainage system (Fig. 1). The Todd Avenue gauge is immediately downstream of a storm drain outfall on the Todd Avenue tributary to Moores Run. Flow from the Todd Avenue tributary enters the main stem of Moores Run at the Moores Run storm drain outfall above the Radecke Avenue stream gauge (Fig. 1).

The 13 June 2003 flood, like most floods in Moores Run, was produced by an organized system of thunderstorms. The storm produced large rainfall rates over the Moores Run catchment for a period of approximately 30 min. Analyses of the 13 June 2003 storm, which are based on volume scan reflectivity observations from the Sterling, Virginia, Weather Surveillance Radar-1988 Doppler (WSR-88D) radar, are used to characterize the spatial and temporal variability of flash flood–producing rainfall and to examine the structure and evolution of flash flood–producing storms. Storm properties are compared with those of five other flash flood–producing storms, which occurred on 21 April and 13 May 2000, 3 August 2002, and 12 June and 6 July 2003. The 2000 and 2002 storms produced annual flood peaks at one or both of the USGS stream gauging stations in Moores Run (Table 1). The 2003 storms produced flood peaks that exceeded the magnitudes of most annual peaks in Moores Run. Like the 13 June 2003 storm, each of the five floods was produced by warm season thunderstorm systems.

Hydrology of flood response in Moores Run is characterized by highly efficient concentration of runoff through the storm drain network and relatively low

TABLE 1. Peak unit discharge (i.e., peak discharge in $m^3 s^{-1}$ divided by drainage area in km^2) for Moores Run at Radecke Ave. (column 2) and Todd Ave. (column 5). Storm total rainfall (mm) and runoff ratio (ratio of basin-averaged runoff to storm total rainfall) are shown in columns 3 and 4 for Moores Run above the Radecke Ave. gauging station. Runoff ratio could not be computed for the 13 Jun 2003 and 3 Aug 2002 event, because only peak stage was available (see additional discussion in text).

	Radecke			Todd
Event	Peak ($m^3 s^{-1} km^{-2}$)	Rain (mm)	Ratio	Peak ($m^3 s^{-1} km^{-2}$)
13 Jun 2003	25.2	46.7	NA	13.7
3 Aug 2002	12.8	47.7	NA	12.1
6 Jul 2003	9.8	37.6	0.42	6.5
12 Jun 2003	6.9	64.9	0.36	2.2
13 May 2000	5.9	20.5	0.35	2.8
21 Apr 2000	2.6	12.7	0.35	11.8

runoff ratios. Most of the basin was developed prior to the implementation of storm water management regulations and there are no significant stormwater detention structures in the basin. The upper 60% of the Moores Run basin above the Radecke Avenue gauge has no surface drainage. The hydrologic response of Moores Run for the 13 June 2003 event is reconstructed using a distributed hydrologic model (Morrison and Smith 2001; Giannoni et al. 2003; Zhang and Smith 2003) and high-resolution rainfall observations derived from radar and rain gauge observations. Hydrologic modeling analyses are also used to examine the dependence of flood response in Moores Run on the time distribution of rainfall.

A detailed survey of high-water marks for the 13 June 2003 flood was carried out immediately following the event. These observations are used, in combination with analyses based on a 2D, depth-averaged hydraulic model (TELEMAC 2D; see Hervouet and Petitjean 1999; Horritt and Bates 2002; Nelson et al. 2004; see also Miller 1995 and Turner-Gillespie et al. 2003) to examine hydraulics of the 13 June flood. Hydraulic analyses are used to examine peak discharge for the 13 June flood peak (the stream gauge was rendered inoperative by the flood), propagation and attenuation of flood waves in the Moores Run channel, and 2D flow features associated with channel and floodplain geometry (especially constrictions and expansions due to bridges, embankments and natural variations in valley bottom geometry).

2. Hydrometeorology of extreme floods in Moores Run

The annual 2003 rainfall in Baltimore of 1574 mm is the largest on record, breaking the previous mark set in 1889. During the 6-month period from 1 April to 30 September 2003, there were 12 events with peak discharge exceeding 1 $m^3 s^{-1} km^{-2}$ in Moores Run. The peak discharge at the Radecke Avenue gauge (Table 1) for the 13 June 2003 flood was estimated to be 25.2 $m^3 s^{-1} km^{-2}$, based on the high-water marks (HWMs) at the stream gauge and the rating curve extended beyond the peak direct discharge measurement of 1.5 $m^3 s^{-1} km^{-2}$ (see section 3 for additional analyses of the 13 June peak discharge). The 12 June and 6 July storms (Table 1) produced floods with peak unit discharge values of 6.9 and 9.8 $m^3 s^{-1} km^{-2}$, respectively. These peaks rank among the larger annual flood peaks in Moores Run (Table 1). In this section the spatial and temporal variability of flash flood–producing rainfall in Moores Run is examined through analyses of the 12 June 2003, 13 June 2003, and 6–7 July 2003 storms, as well as storms that occurred on 21 April 2000, 13 May 2000, and 3 August 2002 (Tables 1 and 2). The 2000 and 2002 storms produced annual flood peaks at one or both of the Moores Run stream gauging stations.

Volume scan radar reflectivity observations from the Sterling WSR-88D are used for hydrometeorological analyses of the six storms. The rainfall rate field at time t and location x is denoted $R(t, x)$. The rainfall rate fields are estimated by applying a Z–R relationship ($R = aZ^b$) to reflectivity observations at volume scan times $t_1, t_2, \ldots$ and for spatial locations $x_j; j = 1, \ldots, M$, where M is the number of radar bins and x_j denotes the center of the jth 1° by 1-km radar bin in the domain. The Sterling WSR-88D is approximately 90 km from the Moores Run watershed (see Smith et al. 1996 for discussion of range effects in radar rainfall estimates). Analyses presented in this paper utilize the "convective" Z–R relationship for which $a = 0.0174$ and $b = 0.71$ (Fulton et al. 1998; Smith et al. 1996; Baeck and Smith 1998). The time-interpolated rainfall rate esti-

TABLE 2. From storm total rainfall fields computed over the region, the maximum (column 2) and minimum (column 3) storm rainfall accumulation in the Moores Run basin was computed for each of the six storms. From basin-averaged rainfall rate time series (5-min time interval) covering the 9.1 km^2 Moores Run watershed, the maximum 15-min (column 4), and maximum 30-min rainfall rates were computed for each of the six storms.

Event	Max storm total (mm)	Min storm total (mm)	Max 15-min rain rate ($mm h^{-1}$)	Max 30-min rain rate ($mm h^{-1}$)
13 Jun 2003	59	25	102	76
3 Aug 2002	56	36	72	63
6 Jul 2003	47	28	80	50
12 Jun 2003	71	29	88	62
13 May 2000	23	17	48	37
21 Apr 2000	23	10	39	24

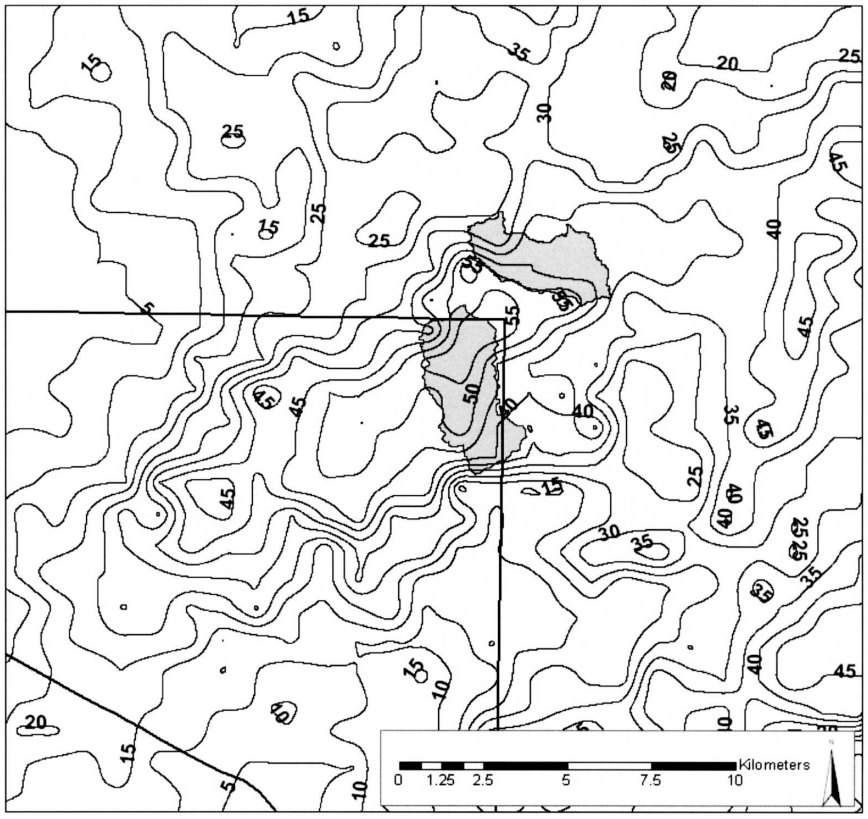

FIG. 2. Storm total rainfall field (mm) for the 13 Jun 2003 storm. The Moores Run and Whitemarsh Run basin boundaries are outlined (Fig. 1), as is the Baltimore City boundary.

mates at radar bin locations are obtained by linear weighting between volume scan times—that is,

$$R(t, x_k) = \frac{t - t_j}{t_{j+1} - t_j} a[Z(t_{j+1}, x_k)]^b + \frac{t_{j+1} - t}{t_{j+1} - t_j} a[Z(t_j, x_k)]^b, \tag{1}$$

for $t_j < t \leq t_{j+1}$. This computation provides estimates at an arbitrary time t, but for locations fixed to the center of radar sample bins x_k. The radar rainfall estimate for time t and location x, $R(t, x)$, is obtained by an inverse distance-squared weighting of the observations from radar bins:

$$R(t, x) = \sum_{k=1}^{M} w_k R(t, x_k) \tag{2}$$

for

$$w_k = \frac{\dfrac{1}{\|x - x_k\|^2}}{\displaystyle\sum_{j=1}^{M} \frac{1}{\|x - x_j\|^2}}. \tag{3}$$

Tipping-bucket rain gauge observations from stations (Fig. 1) in and adjacent to the watershed were provided by Baltimore City Department of Public Works. These observations are used, along with radar reflectivity observations, for rainfall analyses.

The 13 June 2003 flooding in Moores Run was produced by 47 mm of rainfall, averaged over the basin (Fig. 2). Storm total rainfall was greatest in the upper portion of the basin with a maximum of 59 mm in the center of the upper basin. Storm total accumulations decreased to the northwest and southeast, with 25-mm accumulation at the southern end of the basin. The storm produced the record flood peak (18.7 $m^3 s^{-1} km^{-2}$) in Whitemarsh Run (USGS ID 01585090; drainage area of 7.1 km^2), which is located at the northeastern edge of the axis of peak storm total rainfall (Figs. 1 and 2). The Whitemarsh gauging station has a record extending back to 1995. Severe flood damage was also reported in the Herring Run watershed, which is immediately southwest of Moores Run (Fig. 2).

The peak rainfall rates at the RG2 rain gauge (Fig. 3; see Fig. 1 for gauge location) at 5-, 15-, 30-, and 60-min time intervals were, respectively, 146, 126, 104, and 59 mm h^{-1}. These rainfall rates have return inter-

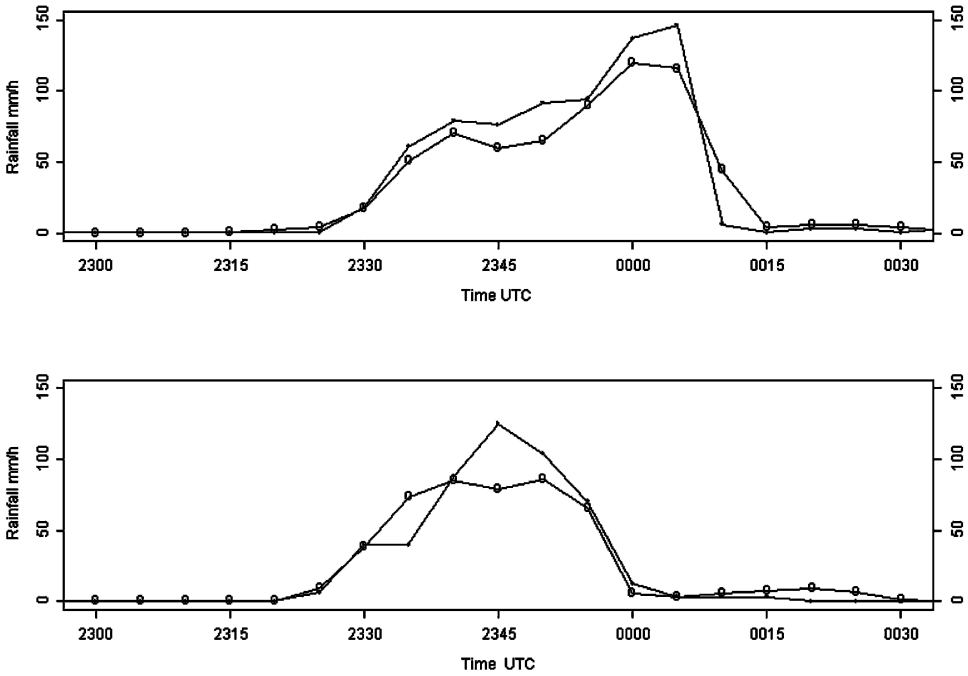

FIG. 3. Time series of rainfall rate (mm h^{-1}) from rain gauge (solid lines) and radar (open circles) at 15-min time increment: (top) RG2 and (bottom) RG5 (see Fig. 1 for locations).

vals (based on NOAA 1961) of 2 (5), 8 (15), 16 (30), and 13 yr (60 min). The 5-min peak occurred during the 0000–0005 UTC time interval on 14 June and the maximum 15- and 30-min rainfall rates all ended at 0005 UTC. Rainfall rate decreased sharply after 0005 UTC (Fig. 3).

Rainfall rate estimates at 5-min time interval computed from WSR-88D reflectivity observations using the convective Z–R relationship were in good agreement with rainfall rate observations from RG2 and RG5 (Fig. 3; see additional discussion of radar estimation of extreme rainfall rates in Baeck and Smith 1998; Uijlenhoet et al. 2003; Smith et al. 2002). There is slight underestimation of peak 5-min rainfall rates. The storm total accumulations of 59.9 mm for RG2 and 41.1 mm for RG5 are matched by radar rainfall estimates at these locations of 55.1 and 39.5 mm. Radar rainfall estimates are used below for examining the spatial variation of storm total rainfall over the Moores Run basin and for examining the temporal variability of basin-averaged rainfall rate. A multiplicative bias correction, based on gauge–radar intercomparisons (see Smith et al. 1996; Baeck and Smith 1998; Fulton et al. 1998) was applied to radar rainfall estimates for the 13 June 2003 storm (and rainfall analyses for the 3 August 2002, 6 July 2003, 12 June 2003, 13 May 2000, and 21 April 2000 storms; see Table 2).

The 13 June 2003 storm (Fig. 4) was a multicell thunderstorm system (Houze 1993). Flooding in Moores Run and surrounding areas was produced during a period of explosive growth of the system from 2332 to 0002 UTC (Fig. 4). At 2332 UTC, a line of rainfall extended from the western boundary of Baltimore City through the northeastern corner of the city (corresponding to the region containing reflectivity values greater than 45 dBZ in Fig. 4). The line was comprised of three cells. The cell at the southwest end of the line had the largest reflectivity values aloft, with peak reflectivity values of 51.5 dBZ between 6 and 7 km AGL (above ground level). The decaying cell in the northeastern corner of the city produced the initial period of rainfall in Moores Run (see Fig. 3 for a time series of rainfall rate). As the southwestern cell entered a downdraft-dominated phase from 2332 to 2342, the surface rain area grew rapidly (Fig. 4). Motion of the storm cells was from west-southwest to east-northeast (60 degrees from North) at an average speed of 40 km h^{-1}.

Growth and decay of a single cell embedded in the system was directly linked to the most extreme rainfall rates over Moores Run (Fig. 5; see also Figs. 2–4). Growth of the cell from 2332 to 2352 resulted in peak reflectivities of 66.5 dBZ (a value characteristic of large hail; see Witt et al. 1998) between 6 and 8 km AGL. The cell collapsed (Fig. 5) over Moores Run during the following 15 min, producing the peak rainfall rates over the region (Fig. 3).

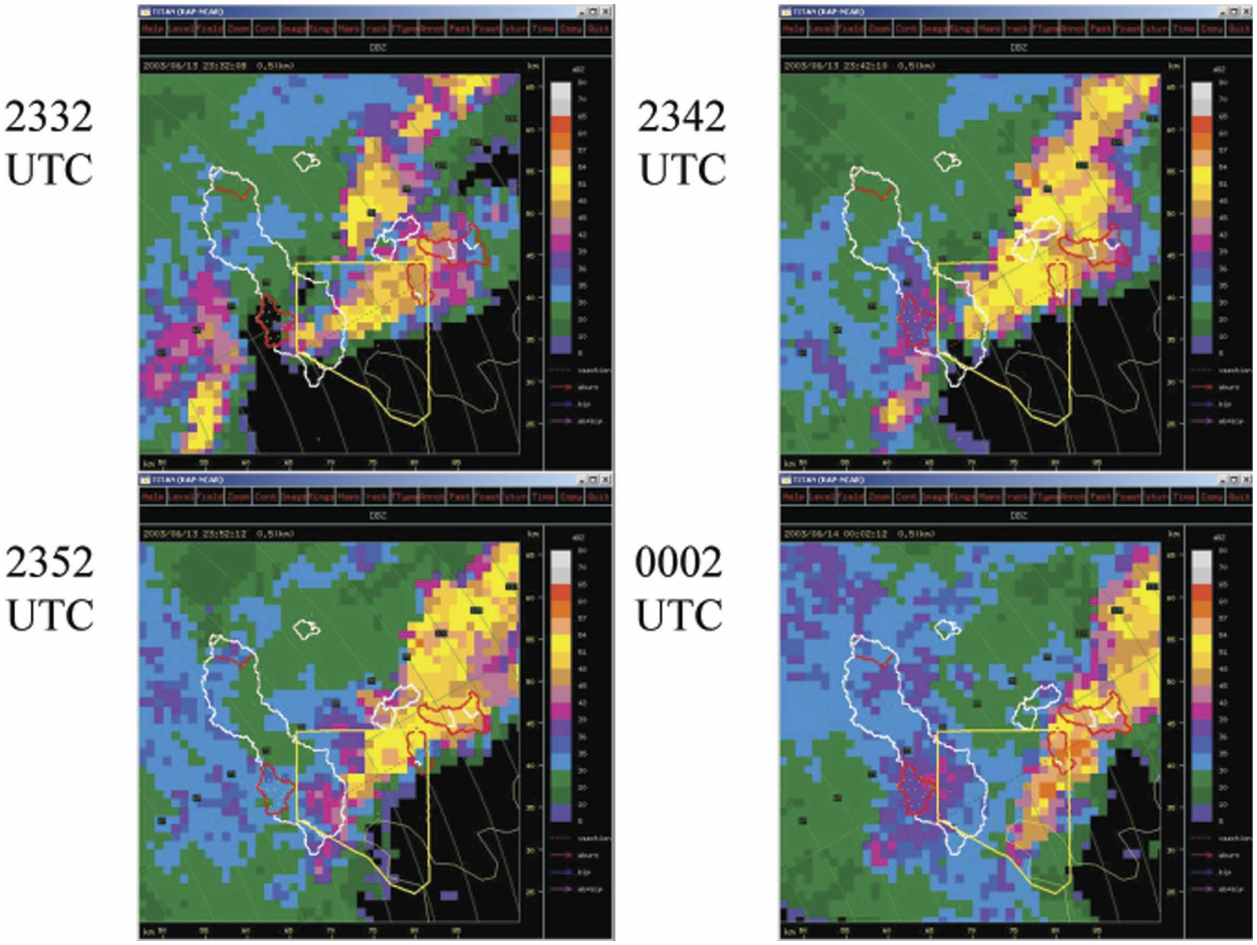

FIG. 4. Low-level reflectivity for the 13 Jun 2003 storm from the Sterling WSR-88D at 2332, 2342, 2352, 0002 UTC 13 and 14 Jun 2003. The Moores Run basin boundary is outlined in red and the Baltimore City boundary is outlined in yellow.

The storm produced large cloud-to-ground flash densities (Fig. 6), with a peak flash density of 10 CG strikes km^{-2} on the western boundary of Moores Run (cf. with climatological analyses in Orville and Silver 1997). Peak lightning production occurred during the period of rapid growth of the cell with a maximum flash rate of nine strikes per minute at 2353 UTC. The lightning chronology of the storm is consistent with the interpretation that peak rainfall rates over Moores Run were closely linked to the downdraft-dominated cycle of the storm cell (Goodman et al. 1988).

Storms producing large flood peaks in Moores Run are, in general, multicell thunderstorm systems, which produce large rainfall rates for short time intervals and with large spatial gradients (Tables 1 and 2). Rainfall fields were computed for the 12 June 2003, 6 July 2003, 3 August 2002, 21 April 2000, and 13 May 2000 storms in similar fashion to rainfall analyses for the 13 June 2003 storm. Rainfall fields for each event are summarized in Table 1 by the mean storm total accumulation over the basin. The maximum and minimum storm total accumulations over the 9.1 km^2 basin and the maximum 15-min and 30-min basin-averaged rainfall rate are given in Table 2). Flood summaries for these events (Table 1) include peak discharge at both Moores Run gauging stations and water balance analyses for the basin above Radecke Avenue. The latter analyses are presented for the events (21 April 2000, 13 May 2000, 12 June 2003, and 6 July 2003) for which continuous discharge observations were available at the Radecke Avenue gauging station. For the two largest peaks, the gauging station was rendered inoperative by flooding, and only peak discharge estimates are available.

Storm evolution on the 30 min cycle of convective cell growth and decay plays a central role in the flood hydrology of Moores Run. The 3 August 2002 storm, which produced a flood peak of 12.8 $m^3 s^{-1} km^{-2}$ at the Radecke Avenue gauge (Table 1), was a rapidly moving multicell storm system. The 15-min period of heav-

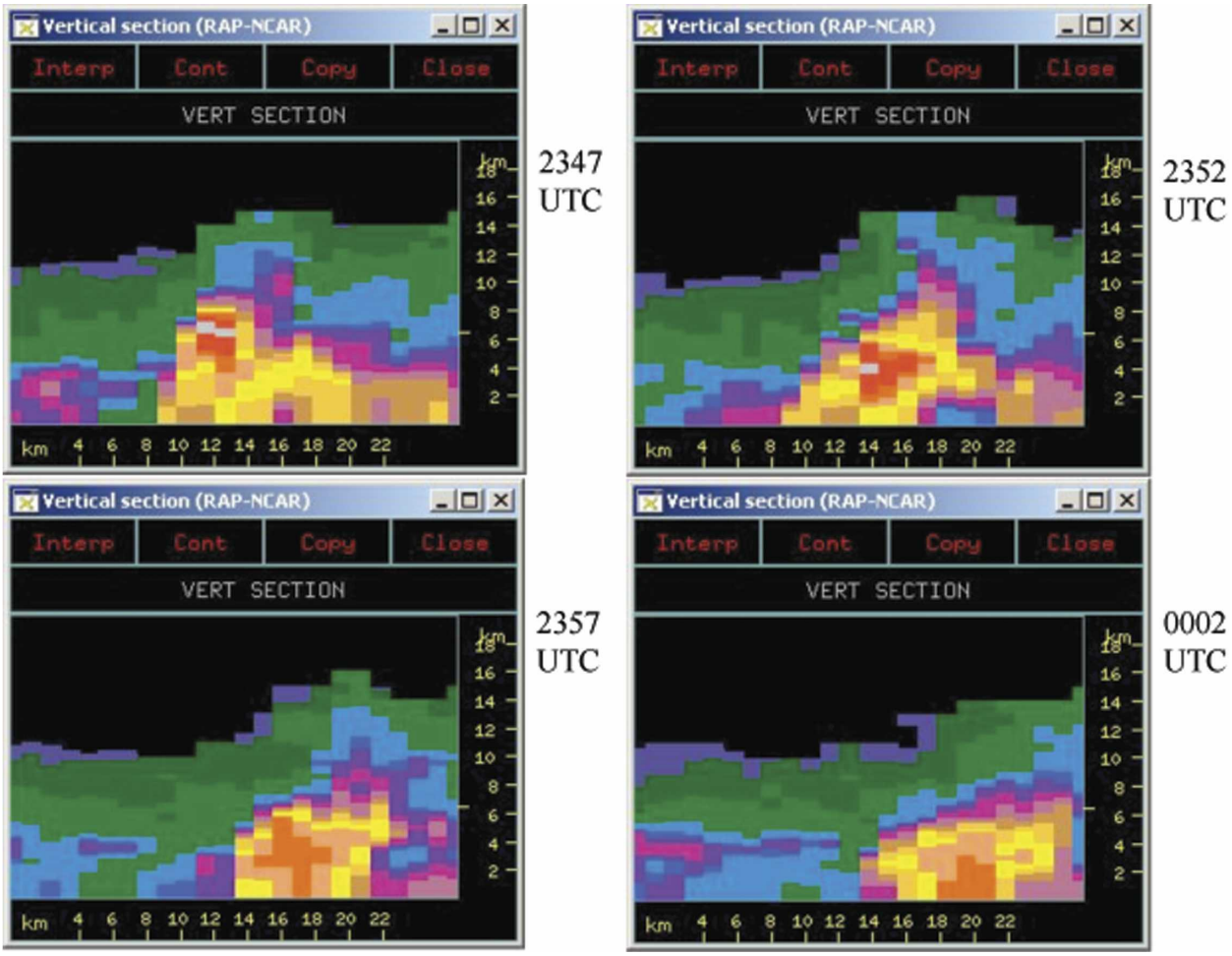

FIG. 5. Vertical profile along the red dashed line in Fig. 4 at 2347, 2352, 2357, and 0002 UTC 13 and 14 Jun 2003.

iest rainfall over Moores Run (Table 2) was preceded by a sharp decrease in the elevation (and magnitude) of the maximum reflectivity in the storm. The elevation of maximum reflectivity decreased from 6–7 km at 0605 UTC (magnitude of 61.5 dBZ) to 3–4 km AGL at 0610 UTC (magnitude of 60.5 dBZ) and 0–3 km AGL at 0616 UTC (magnitude of 59.5 dBZ). The decaying phase of the storm produced a rainfall maximum over Moores Run with large spatial gradients (Fig. 7).

The 6–7 July 2003 storm produced a peak discharge of 9.8 $m^3 s^{-1} km^{-2}$ at Radecke Avenue (Table 1) from a short period of heavy rainfall (Table 2), which resulted in a storm total rainfall accumulation of 37.6 mm (Table 1). Peak reflectivities greater than 50 dBZ at 8 km AGL were observed between 0140–0150 UTC (7 July), when the storm was west of the Moores Run basin. Peak reflectivities at 8 km AGL had decreased to 35 dBZ at 0200 UTC (7 July) and the 50-dBZ level had dropped below 5 km AGL. The decaying cell produced a peak rainfall accumulation of 48 mm along the eastern boundary of the basin (figure not shown; see Table 2). Peak CG flash density of 9 strikes km^{-2} was located in Moores Run, southwest of the rainfall maximum (figure not shown).

Large spatial variation in rainfall over the 9.1 km^2 spatial scale of the Moores Run basin is the rule rather than the exception for flash flood–producing storms. Spatial variability of rainfall can result in large gradients in flood response over the 9.1 km^2 Moores Run basin. The 21 April 2000 storm, which had a maximum rainfall accumulation along a swath passing through the Todd Avenue gauge (Table 2), produced a flood peak at Todd Avenue with a unit discharge flood peak more than 4 times the unit discharge peak at the Radecke Avenue station (Table 1). Measurement error is a significant problem for flood peak estimates in small urban catchments (as discussed further in the subsequent section). The 21 April 2000 event is the only event for which Todd Avenue has a larger unit discharge peak than the Radecke Avenue gauge.

FIG. 6. Storm total cloud-to-ground lightning flash density (strikes km^{-2}) for the 13 Jun 2003 storm.

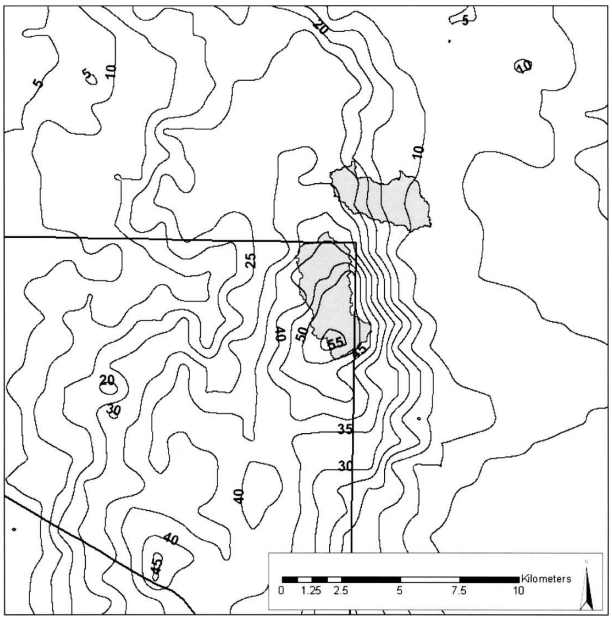

FIG. 7. Storm total rainfall field (mm) for the 3 Aug 2002 storm.

Hydrologic response times in Moores Run are short. The time between peak rainfall rate and peak discharge for the 6–7 July 2003 storm at 9.1 km^2 scale was approximately 15–20 min (Fig. 8). For the 0.51 km^2 scale of the Todd Avenue gauging station response time was 5–10 min. Variability of rainfall on 1–30 min time scale is of fundamental importance for hydrologic response of Moores Run. The 12 June 2003 storm (Table 2) produced larger accumulations than the 13 June storm at the 2 h time scale, but rainfall was organized into a series of pulses of intense rainfall rates. Storm cells repeatedly formed and tracked over the region, a common recipe for flash flooding (see Chappell 1986; Doswell et al. 1996). The temporal structure of the 12 June storm produced a series of three flood peaks (6.9, 5.1, and 3.2 m^3 s^{-1} km^{-2}) during a 2-h time period. The maximum flood peak was smaller than the record flood peak less than 24 h later and the 6–7 July flood peak (Fig. 8), despite larger rainfall accumulations over a 2-h time scale.

Not only is the Moores Run response rapid, but "dispersion" of the hydrograph is small, relative to the time distribution of rainfall (Fig. 8). The 13 May 2000 storm, which produced a single, continuous period of heavy rainfall of thirty minutes duration, resulted in a flood hydrograph for which 90% of the storm event runoff was contained within a 30-min time window. The duration of elevated flood response at the Radeke Avenue stream gauging station is comparable to the duration of extreme rainfall over the 9.1 km^2 basin. The response properties of Moores Run at the outfall of the storm drain system, in particular the rapid response times and lack of hydrograph dispersion, are linked to the pronounced flood wave attenuation in the downstream surface channel system, as discussed in the following section.

The high frequency of extreme flood peaks in Moores Run is not linked to anomalously large runoff ratios (Table 1). Although the 6–7 July 2003 storm produced near-record flood peaks in Moores Run, the fraction of rainfall that was converted to runoff was only 42% (Table 1). Estimated runoff ratios for the 12 June 2003, 13 May 2000, and 21 April 2000 storms were clustered around 35%. Downward revision of the upper portion of the rating curve for the Radecke Avenue gauging station (as discussed in the following section) would result in even smaller runoff ratios.

The storm event response of Moores Run can be accurately reproduced with a simple distributed hydrologic model, using the high-resolution rainfall observations (Fig. 9; based on analyses of the 6–7 July 2003 storm and flood). The Network Model (Morrison and Smith 2001; Zhang and Smith 2003; Giannoni et al. 2003; Turner-Gillespie et al. 2003) is a distributed hydrologic model that partitions the drainage basin into hillslope and channel components and represents discharge at the outlet of a drainage basin as

$$Q(t) = \int_A M\left[t - \frac{d_0(x)}{v_0} - \frac{d_1(x)}{v_1}, x\right] dx, \qquad (4)$$

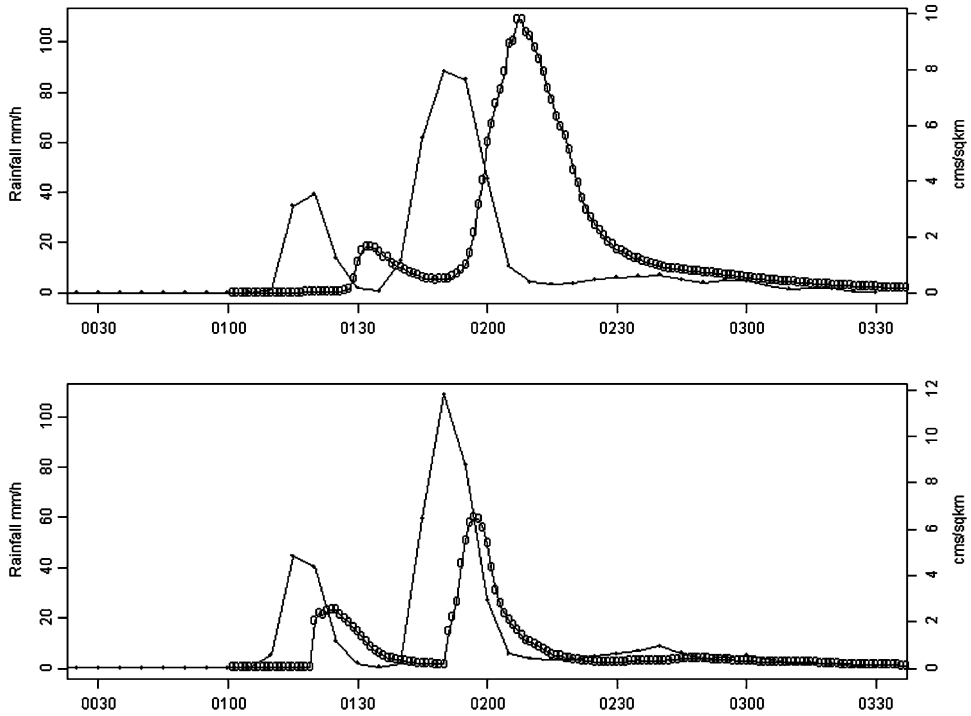

FIG. 8. Basin-averaged rainfall rate (mm h^{-1}; solid lines) and discharge ($m^3\ s^{-1}\ km^{-2}$; open circles) time series for 6–7 Jul 2003 storm at (top) Radecke Ave. and (bottom) Todd Ave.

where $Q(t)$ denotes discharge ($m^3\ s^{-1}$) at time t (s), A is the domain of the drainage basin, x is a point within A, $d_0(x)$ is the distance (m) from x to the channel network (typically, the storm drain network), v_0 is the overland flow velocity ($m\ s^{-1}$), $d_1(x)$ is the distance (m) along the channel from x to the basin outlet, v_1 is the channel flow velocity, and $M(t, x)$ is the runoff rate ($m\ s^{-1}$) at time t and location x. The total flow distance from x to the basin outlet is $d_0(x) + d_1(x)$, the sum of the overland flow distance and the channel flow distance. The runoff rate $M(t, x)$ (mm h^{-1}) at time t and location x is computed from the rainfall rate R(t, x) using the Green–Ampt infiltration model with moisture redistribution (Ogden and Saghafian 1997).

The Network Model was implemented for the Moores Run basin above the Radecke Avenue stream gauge, using a drainage network extracted from a 10-m USGS DEM. The drainage density of the extracted network was designed to represent the density of the storm drain network (see Turner-Gillespie et al. 2003). Network Model parameters for the 6 July event were selected to match the peak magnitude and time of the observed hydrograph and the volume of runoff for a time window centered on the peak time. The resulting parameters were 4.5 m s^{-1} for the channel velocity, v_1,

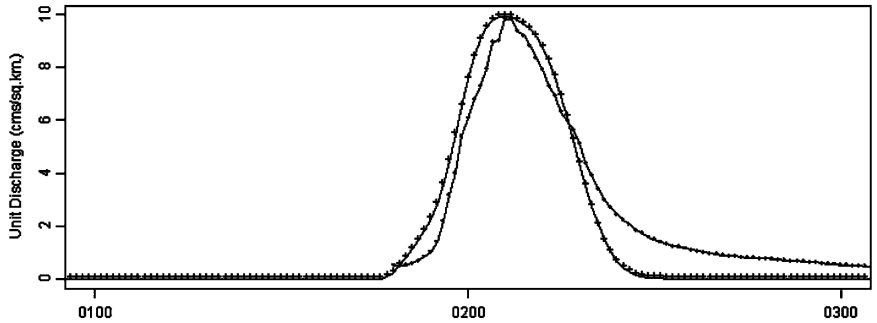

FIG. 9. Network model results for 6–7 Jul 2003 flood. The observed discharge ($m^3\ s^{-1}\ km^{-2}$) is denoted by open circles; the model discharge ($m^3\ s^{-1}\ km^{-2}$) is denoted by "+" symbol.

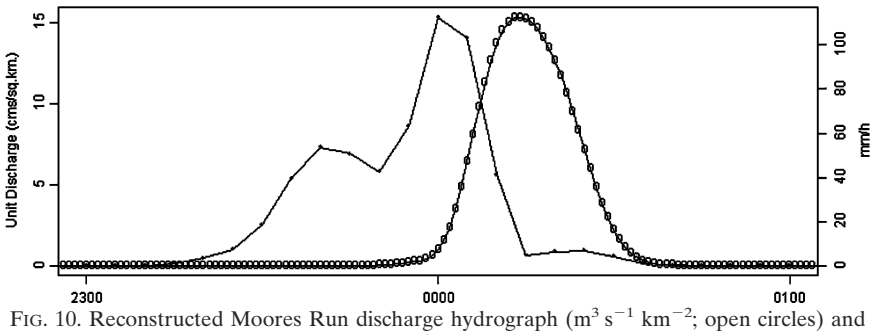

FIG. 10. Reconstructed Moores Run discharge hydrograph ($m^3\ s^{-1}\ km^{-2}$; open circles) and basin-averaged rainfall rate (mm h^{-1}; solid line) for the 13 Jun 2003 storm.

4.5 m s^{-1} for the hillslope velocity v_0, and 2.0 mm h^{-1} for the saturated hydraulic conductivity K_s (the principal soil hydraulic parameter required for the Green–Ampt infiltration equation).

The Network Model parameters reflect the control of the storm drain system on flood response in Moores Run. The channel velocity of 4.5 m s^{-1} is larger than bankfull velocities in natural channels, but it is smaller than the peak velocity of 9 m s^{-1} for which the storm drain outfall is rated. Hillslope velocities are typically 1 or more orders of magnitude smaller than channel velocities. In Moores Run, however, the contributing portion of the watershed is concentrated around the storm drain system. The relatively small runoff ratios (Table 1) for large flood peaks in Moores Run and the small dispersion of Moores Run hydrographs suggest that flood response in Moores Run immediately below the storm drain outfall is controlled by a subset of the basin that is concentrated around the storm drain network and hydraulically connected to the storm drain system. As such, the model velocities account both for the flow velocities in the storm drain system and the restriction of the effective drainage system to a region adjacent to the storm drain system.

The Network Model was used, with parameters calibrated for the 6 July 2003 event and 1 km, 5-min rainfall fields derived for the 13 June 2003 event, to reconstruct the discharge hydrograph for the 13 June 2003 flood (Fig. 10). The model analyses indicate that the time and space distribution of rainfall for the 13 June storm produces a peak discharge, 15.4 $m^3\ s^{-1}\ km^{-2}$; that is, 50% larger than the peak from the 6–7 July 2003 storm. The model-derived peak discharge for the 13 June event is smaller than the peak discharge obtained by extending the rating curve to the observed stage, but larger than the peak discharge inferred from hydraulic analyses in the following section. The time distribution of the 13 June 2003 hydrograph (Fig. 10) is used in the following section to examine flood wave propagation for the 13 June flood.

Flood frequency analyses for urbanizing drainage basins, like Moores Run, are typically complicated by short or nonexistent stream gauging records and time trends in flood response associated with urbanization (see Beighley and Moglen 2003). Hydrologic model analyses were used in conjunction with precipitation frequency products, to examine the upper tail of the flood frequency distribution for Moores Run. For these analyses, spatially uniform rainfall fields with rainfall durations of 5, 15, 30, and 60 min were employed. In each case, the 100-yr rainfall rate was used as the spatially constant rainfall rate. The 5-min 100-yr rainfall rate produced a peak unit discharge of 11.9 $m^3\ s^{-1}\ km^{-2}$. The peak unit discharge increased to 24.9 $m^3\ s^{-1}\ km^{-2}$ for the 15 min, 100-yr rainfall rate and 29.7 $m^3\ s^{-1}\ km^{-2}$ at 30-min time interval. Peak discharge drops sharply to 15.4 $m^3\ s^{-1}\ km^{-2}$ for the 60-min, 100-yr rainfall rate (the 100-yr 60-min rainfall rate, distributed uniformly over the basin, produces the same peak discharge as the 13 June 2003 rainfall field). The extreme flood response of Moores Run is most sensitive to rainfall distribution over a 15–30-min time period. Hydrologic model analyses suggest that the 13 June 2003 storm, which was produced by a storm with 15–30-min time duration produced a flood peak in Moores run, which was approximately 50%–60% of the 100-yr flood peak.

3. Hydraulics of extreme floods in Moores Run

The storm drain network exerts profound controls on Moores Run response, as described in the previous section. Below the storm drain outfall (Fig. 1), channel–floodplain interactions play an important role in flood response. The stream channel below the outfall of the storm drain network is incised and widened relative to preurbanization conditions. The channel–floodplain system in Moores Run is also influenced by alterations of the system associated with road crossings and bridge embankments. In this section, we examine hydraulics of

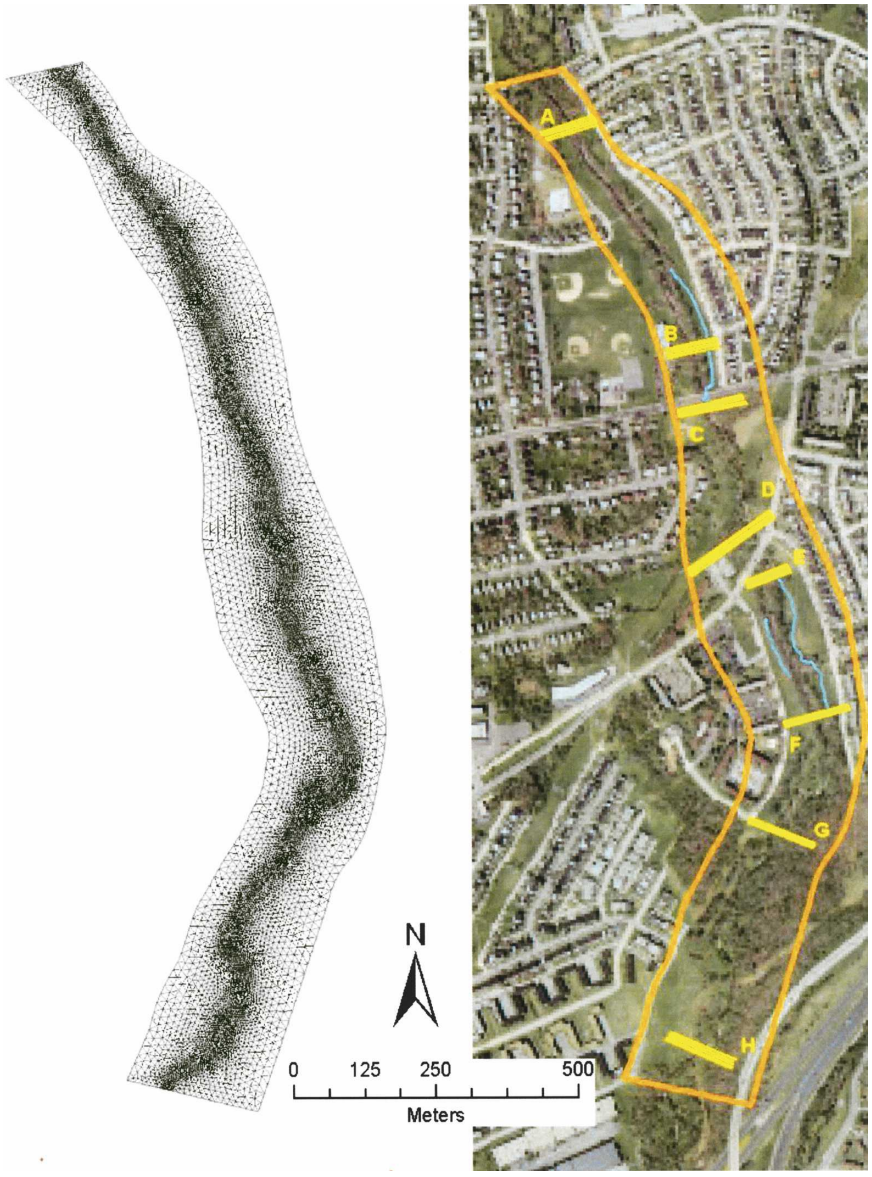

FIG. 11. (right) Aerial photograph of the Moores Run channel reach used for hydraulic model analyses. (left) The finite element mesh used for model analyses. Cross sections for which discharge times series are computed (see Fig. 14) are marked by the letters A–H. The Radecke Ave. Bridge is located between cross sections B and C. The Sinclair Ave. Bridge is located between cross sections D and E. Lines along which dense high-water mark observations were made are shown above Radecke Ave. Bridge and downstream of Sinclair Ave. Bridge.

extreme floods in Moores Run. Of particular interest are 1) hydraulic analyses of peak discharge for the 13 June 2003 flood, 2) analyses of flood wave attenuation and propagation in the surface channel system of Moores Run, and 3) 2D features of the water surface and velocity fields for extreme floods.

A survey of HWMs was carried out on 14–15 June 2003, providing observations adjacent to the Radecke Avenue gauging station and for several stream reaches upstream and downstream of the Radecke Avenue gauge (Fig. 11). Dense surveys of HWMs were performed above the Radecke Avenue Bridge and below the Sinclair Avenue Bridge (Fig. 11).

Channel and floodplain topography were derived from a high-resolution (1 m) LiDAR dataset (vertical accuracy of approximately 10–15 cm), which was ob-

tained for the entire Moores Run drainage basin. Detailed surveys of the Moores Run channel and floodplain were carried out during the summer of 2003 and spring of 2004. The survey and LiDAR data were combined to develop high-resolution topographic data for the Moores Run channel and floodplain (Fig. 11).

Hydraulic analyses of the 13–14 June 2003 flood are based on a 2D depth-averaged model of open channel flow, TELEMAC 2D (Hervouet and Petitjean 1999; Horritt and Bates 2002; Nelson et al. 2004). The depth-averaged momentum equations are given by

$$\frac{\partial u}{\partial t} + u\frac{\partial u}{\partial x} + v\frac{\partial u}{\partial y} = -g\frac{\partial h}{\partial x} - g\frac{\partial z_b}{\partial x} - \frac{1}{\cos\alpha}\frac{gn^2}{h^{(4/3)}}(u^2 + v^2)^{(1/2)}u + \frac{1}{h}\nabla\cdot[h\nu_t\nabla u] \quad (5)$$

$$\frac{\partial v}{\partial t} + u\frac{\partial v}{\partial x} + v\frac{\partial v}{\partial y} = -g\frac{\partial h}{\partial y} - g\frac{\partial z_b}{\partial y} - \frac{1}{\cos\alpha}\frac{g\,n^2}{h^{(4/3)}}(u^2 + v^2)^{(1/2)}v + \frac{1}{h}\nabla\cdot[h\,\nu_t\,\nabla v], \quad (6)$$

where (u, v) is the depth-averaged velocity vector (m s^{-1}), h (m) is the water depth, z_b (m) is the bottom elevation, n is the Manning's roughness parameter, α is the channel slope, and ν_t (m^2 s^{-1}) is the turbulent viscosity. The continuity equation is given by

$$\frac{1}{h}\frac{Dh}{Dt} = -\nabla\cdot(u, v). \quad (7)$$

The turbulent viscosity parameter is specified either as a constant or through the k–ε turbulence model (Rodi 1993). The finite element mesh for the Moores Run reach (Fig. 11) contains 11 158 nodes and 22 017 elements. A flux boundary condition is specified at the upstream end of the reach, near the storm drain outfall. A constant head boundary condition was applied at the downstream end of the reach. The downstream boundary condition has little or no effect on model analyses presented below (location of the boundary was chosen to be far enough downstream of locations for which analyses would be utilized).

The stream gauge at Radecke Avenue was rendered inoperative by the 13 June 2003 flood and peak stage is the only observation for the 13 June flood. As noted above, the peak discharge that is obtained from extension of the rating curve to the peak stage is 25.2 m^3 s^{-1} km^{-2}. Surveyed HWMs were used in conjunction with model analyses to reconstruct the peak discharge for the 13 June flood. The value of peak discharge that best reproduces HWM profiles from model analyses is 13.2 m^3 s^{-1} km^{-2} (Figs. 12 and 13). This result is based on steady state analyses with the k–ε turbulence model and a constant Manning's roughness, n, of 0.035. Reconstructions of peak discharge with a 1D hydraulic model (HEC-RAS) and variable roughness coefficients were carried out independently and resulted in a very similar peak discharge estimate. Ongoing studies are examining the sensitivity to spatially varying roughness in the 2D modeling framework (see also Miller and Cluer 1998 for discussion of sensitivity of 2D model results to variability in roughness).

The reconstructed flow field at 13.2 m^3 s^{-1} km^{-2} discharge in the reach above the Radecke Avenue Bridge (Fig. 12) has flow transitions in the entrance of the reach and at the bridge, but is otherwise gradually varying in both downstream and cross-sectional directions. The observed and modeled HWMs are in good agreement for the reach with a peak discharge of 13.2 m^3 s^{-1} km^{-2} (Fig. 13).

The overestimation of the 13–14 June 2003 flood peak that results from extending the rating curve is due in part to the complex hydraulics in the vicinity of the Radecke Avenue Bridge. Model analyses show superelevation of the free water surface on the right bank of Moores Run at the gauge location (downstream of the Radecke Avenue Bridge). Superelevation of the free water surface results from curvature of the channel–valley bottom flow system in the vicinity of the bridge (Fig. 12).

Many record flood peaks at USGS stream gauging stations, especially in small urban catchments, are based either on extrapolation of the rating curve far beyond the largest direct discharge measurement (Potter and Walker 1985) or indirect discharge measurements. Direct discharge measurements at high flow for stations like Radecke Avenue are virtually impossible. The short times to peak make it difficult to reach the site at or near peak discharge. The rapid rise and fall of the hydrograph translates into a requirement to make velocity measurements at all depths and locations in several minutes. Indirect discharge techniques using detailed surveys of HWMs and 2D hydraulic models provide an important option for specifying the upper tail of the rating curve for stations like Radecke Avenue.

Model analyses suggest that revisions to the Moores Run rating curve will result in lower flood peaks for the 3 August 2002 and 6–7 July 2003 events (Table 1). Revisions to the rating curve diminish as flood peaks de-

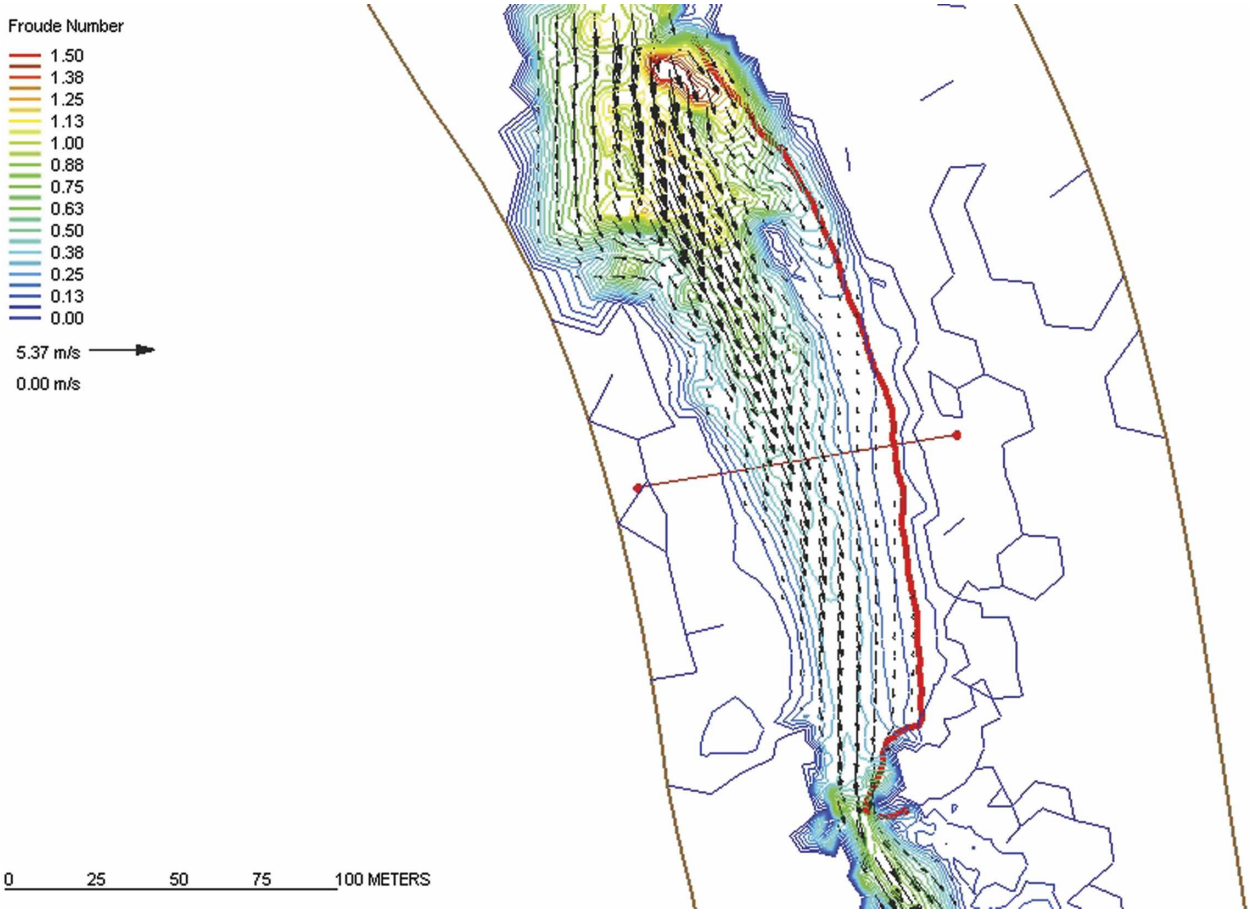

FIG. 12. Flow field above the Radecke Ave. Bridge for the 13 Jul 2003 flood at peak discharge. Arrows denote depth-averaged velocity vectors and the flow field is represented by the Froude number.

crease below bankfull discharge. Even for the 12 June 2003 and 13 May 2000 events, it is likely that flood peaks will be reduced somewhat. Reducing the flood peaks for these events presents an even greater challenge in explaining the relatively low runoff ratios for Moores Run, as discussed in the previous section.

Flood response in Moores Run changes markedly from the storm drain system to the surface channel network. Moores Run flood peaks at the outlet of the storm drain network reflect tightly concentrated response times. As noted in the previous section, response times are comparable to the rainfall duration. In the surface drainage network, attenuation of the flood wave becomes significant. Transient analyses of flood wave attenuation in the Moores Run channel were performed by specifying upstream boundary conditions in terms of the time-varying discharge hydrograph at the storm drain outfall (Fig. 10). For each of the analyses, the upstream discharge has the same time distribution as the hydrograph obtained from model analyses in the previous section (Fig. 10), but the discharge magnitudes are scaled to have a specified peak discharge.

Attenuation of the flood wave in the 1.85 km reach results in a 33% decrease in peak discharge for a peak at Radecke Avenue of 13.2 $m^3 s^{-1} km^{-2}$ (Fig. 14; note that the peak discharge at the upstream boundary is 13.7 $m^3 s^{-1} km^{-2}$ accounting for the attenuation between the storm drain outfall and Radecke Avenue). The dominant controls on flood wave attenuation are storage effects associated with constrictions and expansions of the valley bottom (Fig. 15). The largest attenuation is due to the relatively low relief valley bottom on the right side of the valley upstream of the Sinclair Avenue Bridge (Fig. 11). Significant attenuation is also seen at the Radecke Avenue Bridge constriction and "natural" constriction–expansion reaches (Fig. 15).

The magnitude of flood wave attenuation in the Moores Run channel system does not exhibit large variations with peak discharge. Model analyses were carried out for a series of cases in which the time dis-

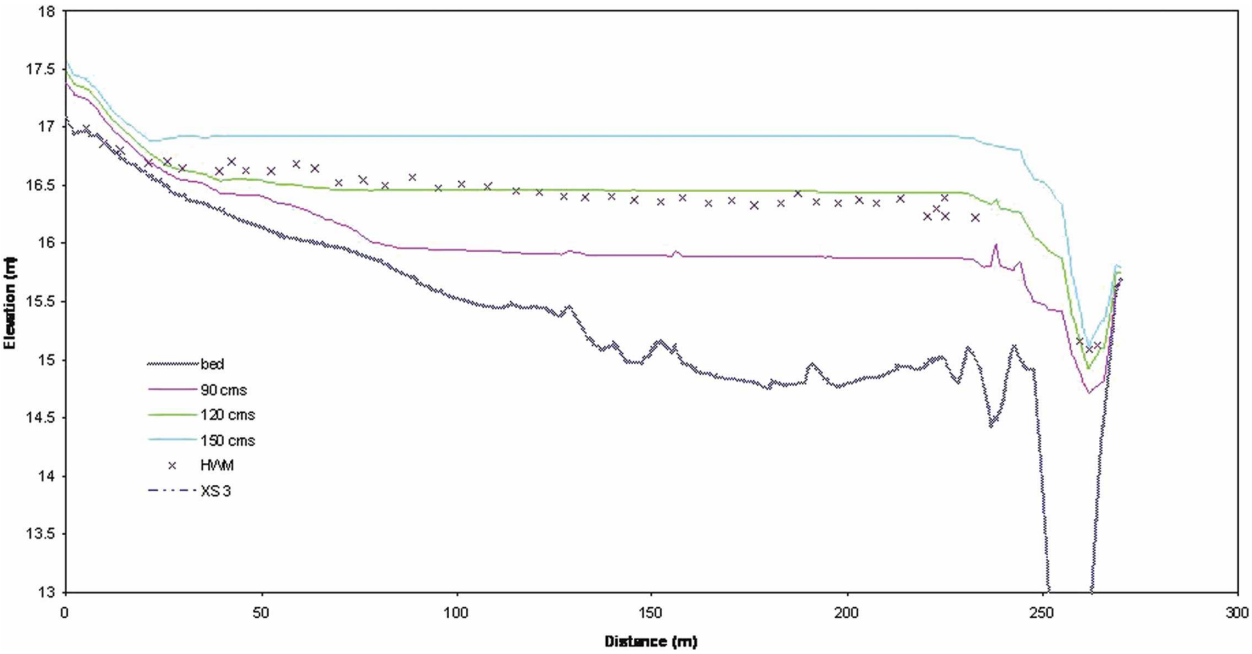

FIG. 13. Observed high-water marks (denoted by the symbol "x") and model free water surface above the Radecke Ave. Bridge (see Figs. 11 and 12). Model free water surface is shown for peak discharge values of 90, 120, and 150 $m^3 s^{-1}$ (9.9, 13.2, and 16.5 $m^3 s^{-1} km^{-2}$). Vertical lines correspond to the marked cross section in Fig. 12.

tribution of discharge was identical to the 13 June 2003 hydrograph, but for which discharge values were scaled so that peak discharge took values ranging from 1.5 to 25.2 $m^3 s^{-1} km^{-2.}$ The lower bound corresponds to a discharge close to the maximum value for which a direct discharge measurement has been made (and consequently, the rating curve is well defined). The upper bound corresponds to the peak discharge for the

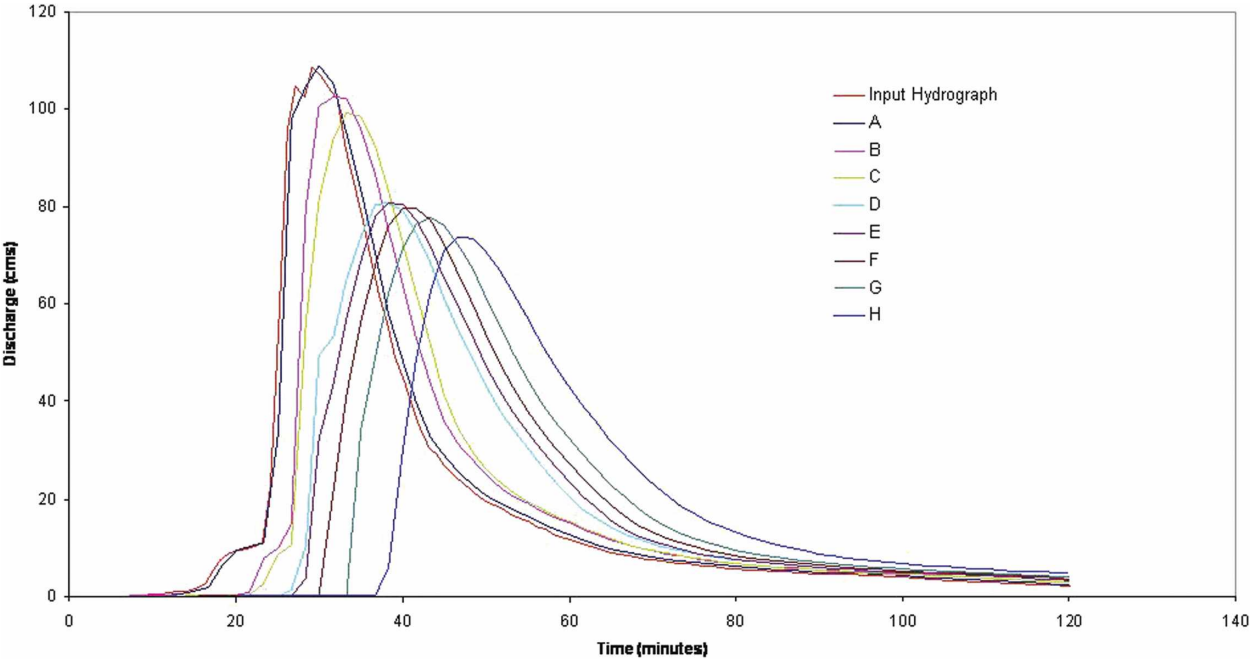

FIG. 14. Discharge time series illustrating flood wave attenuation for 13.2 $m^3 s^{-1} km^{-2}$ peak discharge at Radecke Ave. The hydrographs are for the cross sections labeled A–H in Fig. 11.

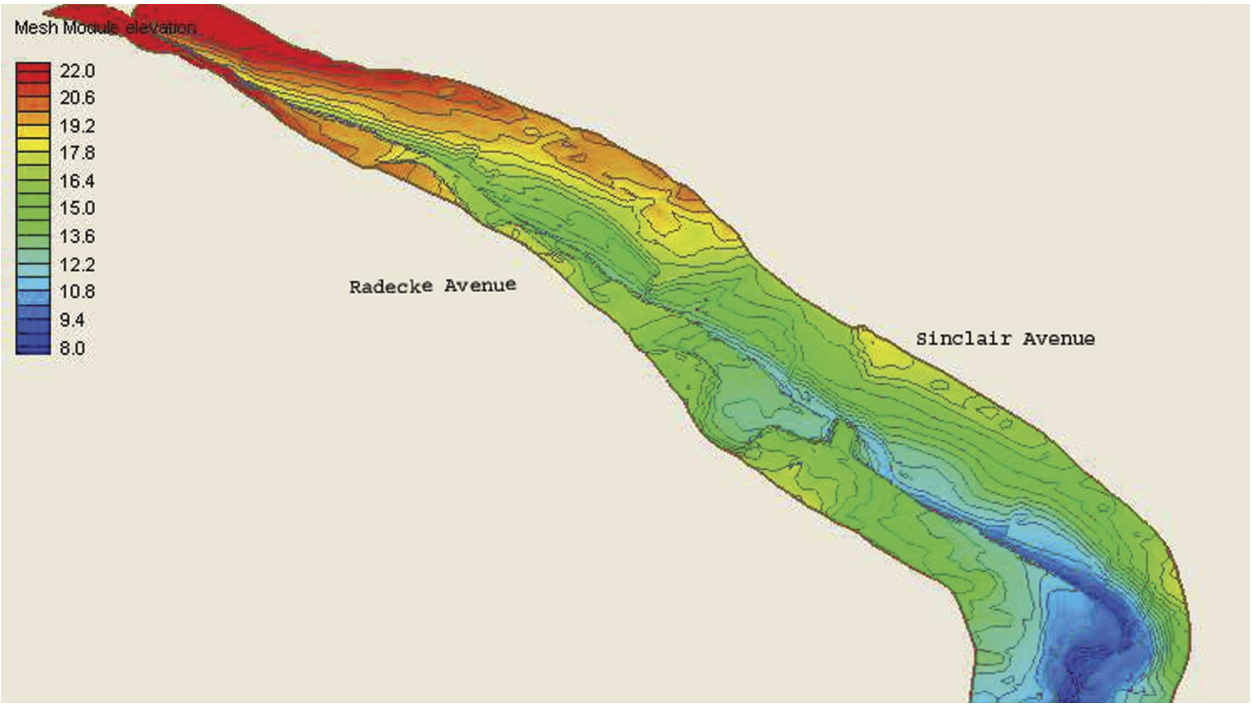

FIG. 15. Topography of Moores Run channel, illustrating major floodplain storage zones including those above the Radecke Ave. Bridge and the Sinclair Ave. Bridge (see Fig. 11).

13 June event that results from extension of the rating curve.

Not surprisingly, flood wave attenuation is large for a peak discharge of 25.2 $m^3 s^{-1} km^{-2}$. The reduction in peak magnitude over the reach is 33% and attenuation is dominated by storage effects above the Sinclair Avenue Bridge. There is also significant peak attenuation for the 1.5 $m^3 s^{-1} km^{-2}$ peak. The magnitude of the peak attenuation, 32%, is only slightly smaller than the magnitude of attenuation for the 25.2 $m^3 s^{-1} km^{-2}$ case. Attenuation for the 1.5 $m^3 s^{-1} km^{-2}$ case, however, is distributed more uniformly over the channel reach, with a much smaller impact of the Sinclair Avenue Bridge. The attenuation effects of the Sinclair Avenue Bridge become prominent for peak upstream discharge between 3 and 6 $m^3 s^{-1} km^{-2}$.

The flood response times in Moores Run are slower for the channel–floodplain system than for the upstream portion of the basin which is controlled by the storm drain network. Time from peak rain rate to peak discharge at Radecke Avenue was shown in the previous section to be 15–20 min. This time scale and the characteristic flow velocities associated with this response time (see previous section) are representative of response from the storm drain system. The time scale for a 13.2 $m^3 s^{-1} km^{-2}$ flood peak to pass through the 1.85 km reach is 17 min (wave speed of 1.85 m s^{-1}). For a peak discharge of 1.5 $m^3 s^{-1} km^{-2}$ the transit time of a flood wave is 26 min and the wave speed is 1.19 m s^{-1}.

Roughness has a pronounced impact on flood wave propagation, including the magnitude of attenuation. Transient runs with peak discharge of 13.2 $m^3 s^{-1} km^{-2}$ were made with uniform roughness values of 0.05 and 0.075, in addition to the baseline run at 0.035. Peak attenuation increased from 33% for $n = 0.035$ to 37% at $n = 0.05$ and 44% for $n = 0.075$. Travel time through the reach increased to 20 min at $n = 0.05$ (wave speed of 1.54 m s^{-1}) and 27 min (wave speed of 1.16 m s^{-1}) for $n = 0.075$. Ongoing studies concern the effects of spatially varying roughness.

The free water surface and depth-averaged velocity fields, as derived from model analyses, exhibited striking cross-sectional and downstream variations. Spatial variations of the free water surface and velocity field are of primary importance for many applications, including estimation of flood peak magnitudes (as discussed above), floodplain mapping and flood inundation forecasting.

The reach downstream of Sinclair Avenue is characterized by a region of supercritical flow (Fig. 16) upstream and into the valley bottom constriction. Channel geometry is asymmetric through the reach with a high bank along the right margin of the channel and a pronounced drop in the left bank, opening the valley bot-

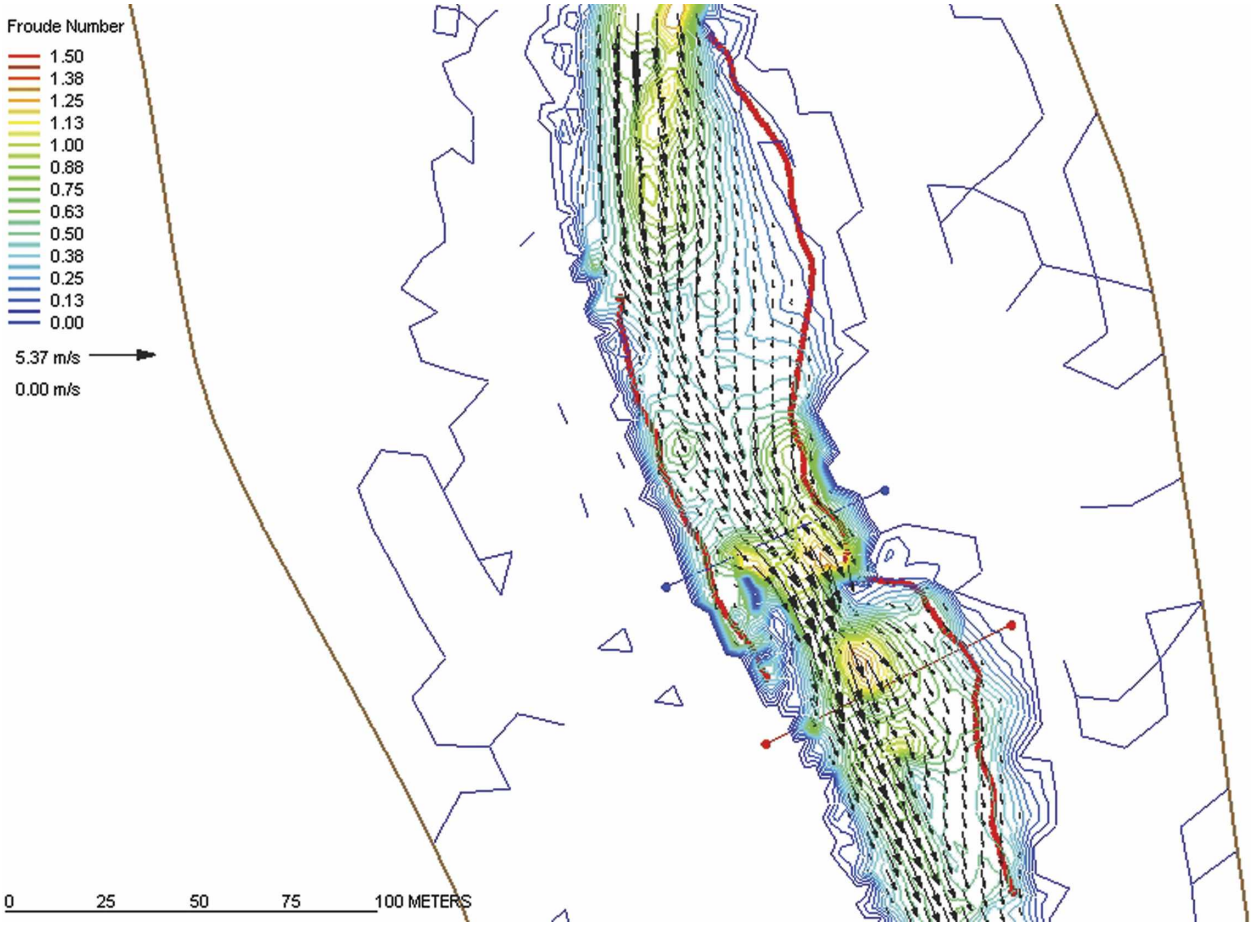

FIG. 16. Flow field below the Sinclair Ave. Bridge at peak discharge. The domain covers the reach between cross sections E and F in Fig. 11 (the extent of the reach can also be seen in Fig. 11 by reference to the lines showing the channel length on left and right banks for which HWM observations were made). Arrows denote depth-averaged velocity vectors and the flow field is represented by the Froude number. Lines across the channel denote the cross sections used in Fig. 18.

tom along the left margin of the channel downstream of the constriction. The asymmetries in the channel–valley bottom geometry, as well as in the prominence of flow transitions, are reflected in the HWMs (Fig. 17). Along the right margin of the channel (Fig. 18, top), overbank flow of approximately 0.5 m extended several meters from the channel margin. The extent and depth of overbank flow decreased toward the downstream end of the reach with very shallow flow extending just beyond the channel margin. These features are reflected both in the observed HWMs and model analyses. The cross-sectional variation in the free water surface at the downstream cross section (Fig. 18, bottom) is more than half a meter (results at the channel margin reflect the wetting and drying algorithm and should be interpreted with caution; see Horritt 2002). The downstream variation of the free water surface (both observed and modeled) along the left margin is dominated by a low channel margin and broader floodplain (Fig. 18, bottom). These features combine to provide an important storage zone for large flood peaks.

The channel–floodplain system in Moores Run has been dramatically altered by more than a century of elevated flood peaks associated with urbanization of the drainage basin. The channel has been widened and incised to accommodate the high frequency of large unit discharge peaks. In the reach downstream of Sinclair Avenue (Fig. 16), it is notable that a flood peak of 13.2 $m^3 s^{-1} km^{-2}$ can be largely accommodated within the channel (Fig. 18). The channel–floodplain system plays an important role in determining the response properties of Moores Run to warm season thunderstorms. In turn, the altered hydrologic regime associated with urbanization has produced a dynamically changing channel–floodplain system that is controlled both by urban infrastructure and the extreme rainfall rates of warm-season thunderstorm systems.

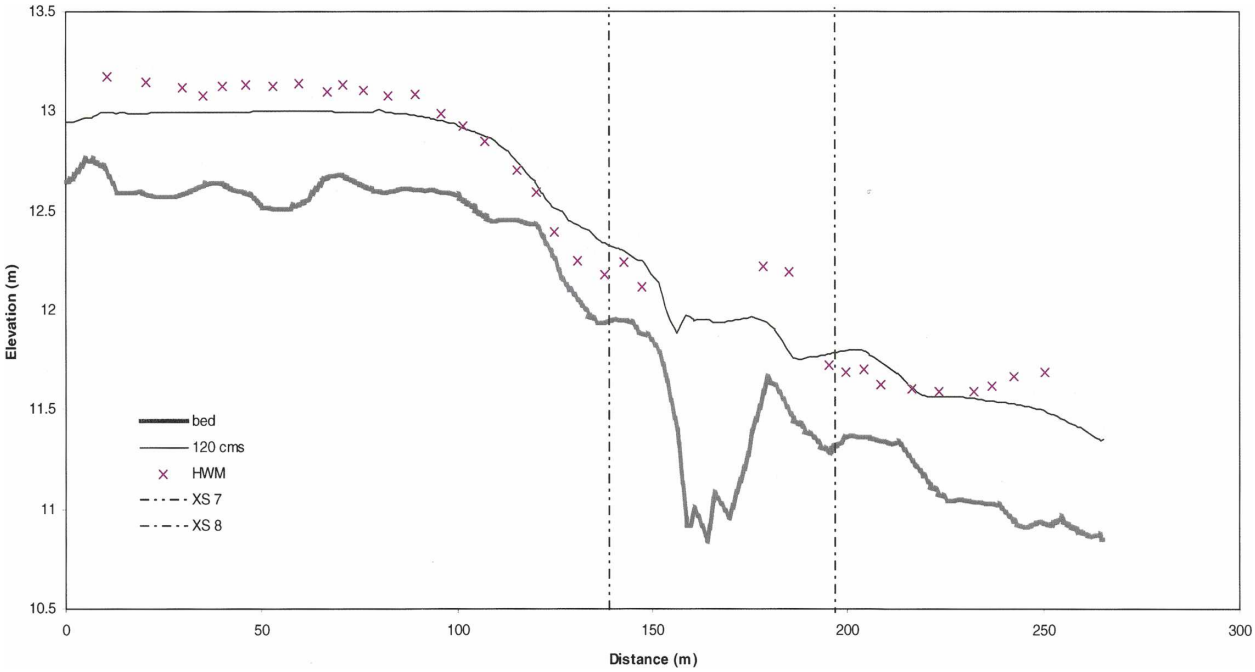

FIG. 17. Observed high-water marks (denoted by "x") and model free water surface for the reach below Sinclair Ave. Bridge (see Figs. 11 and 16). Model free water surface is shown for peak discharge values of 13.2 $m^3 s^{-1} km^{-2}$ at Radecke Ave. Vertical dashed lines show cross sections used in Fig. 18 (see also Fig. 16 for locations of cross sections).

4. Summary and conclusions

The Moores Run watershed in Baltimore City has an exceptionally high frequency of flood peaks exceeding 1 $m^3 s^{-1} km^{-2}$, approximately 12 events yr^{-1}. The hydrometeorology, hydrology and hydraulics of flood response in Moores Run have been examined through analyses of six major flood events in Moores Run. Particular attention is given to the 13 June 2003 event, which produced the record flood peak for the basin. Major conclusions from these analyses are the following.

1) Extreme floods in Moores Run are typically produced by multicell thunderstorm systems. The 13 June 2003 storm was a multicell thunderstorm system that produced 46.7 mm of rainfall over the basin during a 30-min time period.
2) A dense dataset of high-water marks for the 13–14 June 2003 event was collected immediately following the flood. HWM and hydraulic model analyses were used to reconstruct the peak discharge of 13.2 $m^3 s^{-1} km^{-2}$ for the 13 June flood. The peak discharge obtained from extending the rating curve to the observed peak stage is almost twice this value. The combination of dense surveys of HWMs and 2D hydraulic modeling provides an important avenue to pursue in estimating peak discharge for extreme floods, especially in fast-responding urban watersheds.
3) Storm evolution on the 30-min cycle of convective cell growth and decay plays a central role in the flood hydrology of Moores Run. The most extreme rainfall rates in Moores Run at 5–15-min time scale for the 13 June 2003 storm were produced by collapse of a single convective cell over the basin.
4) Large spatial variation in rainfall over the 9.1 km^2 spatial scale of the Moores Run basin is characteristic of flash flood producing storms. Storm total accumulations for the 13 June 2003 storm ranged from a maximum of 59 mm to a minimum of 25 mm. Spatial variability of rainfall can result in large gradients in response over the 9.1 km^2 Moores Run basin.
5) Extreme flood response of Moores Run is not linked to anomalously large runoff ratios. Storm-event runoff ratios (Table 1) are comparable to the impervious fraction of the basin.
6) Rapid response times of Moores Run are paired with very small "dispersion" of the hydrograph. For single-peak flood events, like the 13 May 2000 storm, the rainfall duration is virtually indistinguishable from the duration of the storm event response. A simple distributed hydrologic model was used to reproduce response to the 6–7 July 2003 storm and

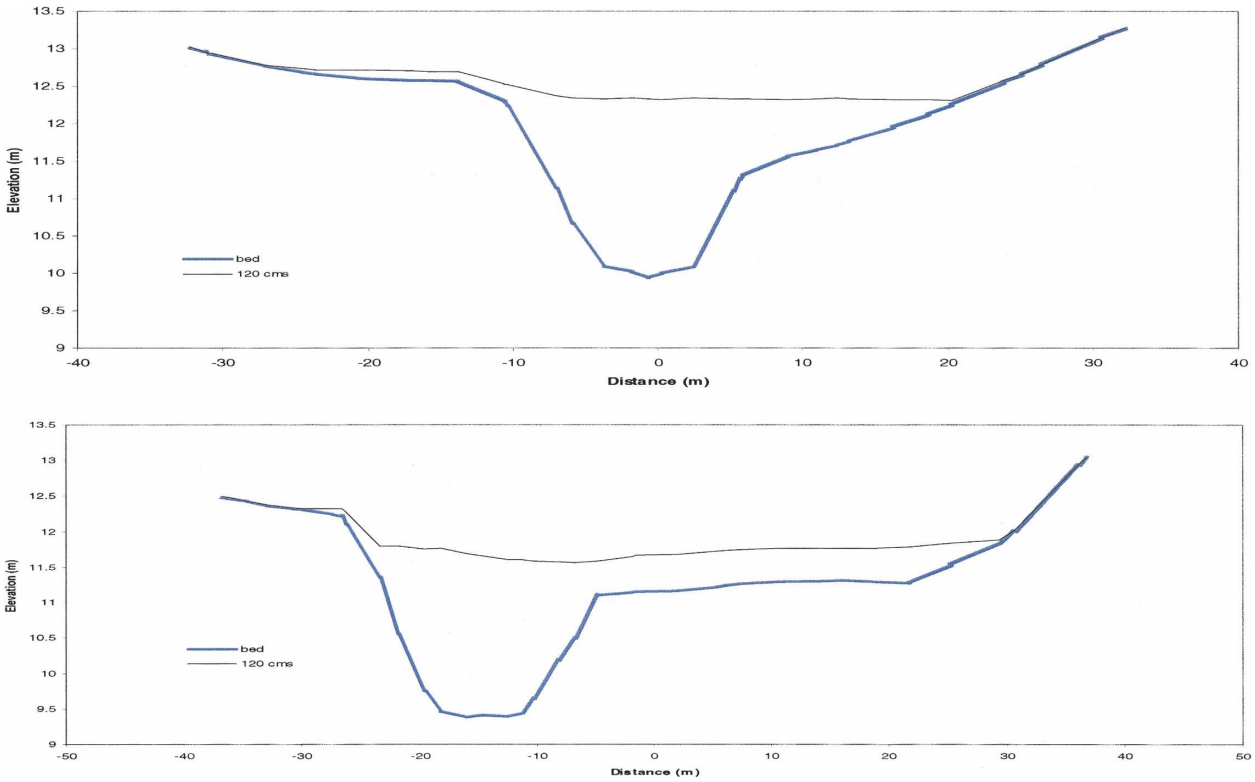

FIG. 18. Cross sections of free water surface at peak discharge for cross section shown in Fig. 16: (top) upstream section and (bottom) downstream section.

reconstruct the hydrograph for the 13 June 2003 event. The characteristic velocities for response from the storm drain system are very large, 4.5 m s^{-1}. The large velocities and relatively small runoff ratios suggest that hydrologic response above the surface channel network is controlled by a subset of the basin, organized around and hydraulically connected to the storm drain system. Model analyses are also used to illustrate the strong dependence of extreme flood response on 15–30-min rainfall rates.

7) Flood peak attenuation for the 13 June 2003 event in the 1.85-km stream reach below the Moores Run storm drain outfall is approximately 33%. Attenuation is largely controlled by constrictions and expansions of the valley bottom. The largest attenuation is associated with a bridge and embankment. Significant attenuation is also associated with natural constrictions and expansions of the valley bottom. Model analyses indicate that the magnitude of peak attenuation is comparably large for peaks up to twice the magnitude of the 13 June 2003 peak, with an increasing influence of storage from a single bridge and embankment. Surprisingly, peak attenuation is also comparable in magnitude for a flood peaks an order of magnitude smaller than the 13 June peak. For the smaller peaks, however, attenuation is distributed more uniformly along the stream reach.
8) The free water surface and depth-averaged velocity fields for extreme floods in Moores Run, as derived from model analyses and intercomparison with surveyed HWMs, exhibit striking cross-sectional and downstream variations. Spatial variations of the free water surface and velocity field are of primary importance for many applications, including estimation of flood peak magnitudes, floodplain mapping and flood inundation forecasting.
9) The channel–floodplain system in Moores Run has been altered by more than a century of elevated flood peaks associated with urbanization of the drainage basin. The altered hydrologic regime associated with urbanization has produced a dynamically changing channel–floodplain system that is largely controlled by the extreme rainfall rates of warm-season thunderstorm systems.

Acknowledgments. The authors would like to acknowledge the assistance of Elliot Holland, Matt Ballantine, and Jane Diehl with data collection and analy-

sis. The research was supported by the National Science Foundation Grants EAR-0208269 and EAR-04090502.

REFERENCES

Baeck, M. L., and J. A. Smith, 1998: Estimation of heavy rainfall by the WSR-88D. *Wea. Forecasting,* **13,** 416–436.

Beighley, R. E. and G. E. Moglen, 2003: Adjusting measured peak discharges from an urbanizing watershed to reflect a stationary land use signal. *Water Resour. Res.,* **39,** 1093, doi:10.1029/2002WR001846.

Chappell, C., 1986: Quasistationary convective events. *Mesoscale Meteorology and Forecasting*, P. Ray, Ed., Amer. Meteor. Society, 289–310.

Doswell, C. A., H. E. Brooks, and R. A. Maddox, 1996: Flash flood forecasting: An ingredients based methodology. *Wea. Forecasting,* **11,** 560–581.

Fulton, R. A., J. P. Breidenbach, D.-J. Seo, D. A. Miller, and T. O'Bannon, 1998: The WSR-88D rainfall algorithm. *Wea. Forecasting,* **13,** 377–395.

Giannoni, F., J. A. Smith, Y. Zhang, and G. Roth, 2003: Hydrologic modeling of extreme floods using radar rainfall estimates. *Adv. Water Res.,* **26,** 195–203.

Goodman, S. J., D. E. Buechler, and P. D. Wright, 1988: Lightning and precipitation history of a microbust-producing storm. *Geophys. Res. Lett.,* **15,** 1185–1188.

Hervouet, J.-M., and A. Petitjean, 1999: Malpasset dam-break revisited with two-dimensional computations. *J. Hydraul. Res.,* **37,** 777–788.

Horritt, M. S., 2002: Evaluation of wetting and drying algorithms for finite element modeling of shallow water flow. *Int. J. Num. Meth. Eng.,* **55,** 835–851.

——, and P. D. Bates, 2002: Evaluation of 1D and 2D numerical models for predicting river flood inundation. *J. Hydrol.,* **268,** 87–99.

Houze, R. A., 1993: *Cloud Dynamics*. Academic Press, 573 pp.

Miller, A. J., 1995: Valley morphology and boundary conditions influencing spatial patterns of flood flow. *Natural and Anthropogenic Influences in Fluvial Geomorphology: The Wolman Volume*, J. E. Costa et al., Eds., *Geophysical Monogr.,* Vol. 89, Amer. Geophys. Union, 57–81.

——, and B. L. Cluer, 1998: Modeling considerations for simulation of flow in bedrock channels. *Rivers over Rock: Fluvial Processes in Bedrock Channels*, K. J. Tinkler and E. E. Wohl, Eds., *Geophys. Monogr.,* Vol. 107, Amer. Geophys. Union, 61–104.

Morrison, J. E., and J. A. Smith, 2001: Scaling properties of flood peaks. *Extremes,* **4,** 5–23.

Nelson, P. A., J. A. Smith, and A. J. Miller, 2004: Evolution of channel morphology and hydrologic response in an urbanizing drainage basin. *Earth Sur. Proc. Landforms,* in press.

NOAA, 1961: Rainfall frequency atlas of the United States for durations from 30 minutes to 24 hours and return periods from 1 to 100 years. NWS Tech. Paper 40, 115 pp.

Ogden, F. L., and B. Saghafian, 1997: Green and Ampt infiltration with redistribution. *J. Irr. Drainage Eng., ACSE,* **123** (5), 386–393.

Orville, R. E., and A. C. Silver, 1997: Lightning ground flash density in the contiguous United States, 1992–1995. *Mon. Wea. Rev.,* **125,** 631–638.

Potter, K. W., and J. W. Walker, 1985: An empirical study of flood measurement error. *Water Resour. Res.,* **21,** 403–406.

Rodi, W., 1993: *Turbulence Models and Their Application in Hydraulics—A State-of-the-Art Review*. 3d ed. International Association for Hydraulic Research, 104 pp.

Smith, J. A., D.-J. Seo, M. L. Baeck, and M. D. Hudlow, 1996: An intercomparison study of NEXRAD precipitation estimates. *Water Resour. Res.,* **32,** 2035–2045.

——, M. L. Baeck, J. E. Morrison, P. Sturdevant-Rees, D. F. Turner-Gillespie, and P. D. Bates, 2002: The regional hydrology of extreme floods in an urbanizing drainage basin. *J. Hydrometeor.,* **3,** 267–282.

Turner-Gillespie, D. F., J. A. Smith, and P. D. Bates, 2003: Attenuating reaches and the regional flood response of an urbanizing drainage basin. *Adv. Water Resour.,* **26,** 673–684.

Uijlenhoet, R., J. A. Smith, and M. Steiner, 2003: The microphysical structure of extreme precipitation as inferred from ground-based raindrop spectra. *J. Atmos. Sci.,* **60,** 1220–1238.

Witt A., M. D. Eilts, G. J. Stumpf, J. T. Johnson, E. D. Mitchell, and K. W. Thomas, 1998: An enhanced hail detection algorithm for the WSR-88D. *Wea. Forecasting,* **13,** 286–303.

Zhang, Y., and J. A. Smith, 2003: Space–time variability of rainfall and extreme flood response in the Menomonee River basin, Wisconsin. *J. Hydrometeor.,* **4,** 506–517.